

# NMR Study of Structure and Dynamics of Ionic Multiplets in Ethylene–Methacrylic Acid Ionomers

Yuanyuan Jia, Alfred Kleinhammes, and Yue Wu\*

Department of Physics and Astronomy and Curriculum in Applied and Materials Sciences, University of North Carolina, Chapel Hill, North Carolina 27599-3255

Received November 15, 2004; Revised Manuscript Received January 20, 2005

**ABSTRACT:** Structural and dynamical properties of ionic multiplets in poly(ethylene-co-methacrylic acid) ionomer neutralized with Na ions were studied by  $^{23}\text{Na}$  nuclear magnetic resonance (NMR) and differential scanning calorimetry (DSC). It was found that the low-temperature peak in DSC spectra is affected by relaxation, compression, and hydration and is related to structure in proximity to ionic multiplets, instead of multiplets themselves. The distance between Na ions in ionic multiplet was determined on the basis of a second moment measurement, suggesting that multiplets are composed of close-packed  $\text{Na}^+\text{--O}^-$  ionic pairs. Motional narrowing of  $^{23}\text{Na}$  NMR line width and transverse relaxation measurement indicate that the time scale of motion of Na or its surrounding is on the order of a few hundred microseconds near room temperature.

## Introduction

Ionomers derived from neutralization of ethylene/methacrylic acid (E/MAA) copolymer, known as Surlyn, possess unique mechanical, rheological, and thermal properties<sup>1–3</sup> as well as the intriguing property of self-healing.<sup>4,5</sup> These ionomers contain typically 15 mol % or less MAA which are partially neutralized with metal cations,<sup>6–9</sup> such as  $\text{Zn}^{2+}$  and  $\text{Na}^+$ . It is believed that aggregation of ionic pairs, such as  $\text{--O}^-\text{--Na}^+$ , plays a crucial role in determining the unique properties of Surlyn.<sup>1–3</sup> Many tools have been used in studying the microstructure of Surlyn, including small-angle X-ray scattering (SAXS),<sup>10–13</sup> differential scanning calorimetry (DSC),<sup>1–3,8,12,13</sup> infrared spectroscopy (IR),<sup>12</sup> and nuclear magnetic resonance (NMR).<sup>1,8</sup> Scattering studies such as SAXS indicate that ionic pairs attract each other forming aggregates, called multiplets.<sup>15</sup> It is generally accepted that there are three regions in Surlyn: polyethylene crystalline lamellae, amorphous matrix, and multiplets of ionic pairs. The formation of ionic multiplets is believed to have a profound influence on the mechanical, thermal, and other physical and chemical properties. Previous DSC studies showed that two endothermic peaks are present upon heating of structurally relaxed (aged) Surlyn. The higher temperature peak, around 90 °C, is attributed to the melting of polyethylene crystalline lamellae.<sup>2,8,12,16</sup> The identity of the low-temperature peak around 50 °C remains unclear. This peak is absent in samples immediately after cooling from the melt and recovers after a certain period of structural relaxation at room temperature.<sup>2,8,12,16</sup> It was found that this low-temperature peak is also affected by hydration<sup>14</sup> and stretching.<sup>13</sup> One of the proposed explanations is the order–disorder transition of the ionic multiplet.<sup>2,16</sup> Others suggest that this peak is associated with the melting of imperfect crystallites of short segment polyethylene or changes occurring in the region surrounding the ionic multiplet rather than the ionic multiplet itself.<sup>13</sup> NMR is a sensitive probe of local structures and dynamics.  $^{23}\text{Na}$  NMR provides a natural probe of the structure and dynamics of ionic

multiplets in E/MAA neutralized by sodium. In this study, NMR and DSC were employed to investigate the structure and dynamics of ionic multiplets. By comparing changes of thermal properties and  $^{23}\text{Na}$  NMR spectra under various sample conditions such as structural relaxation, mechanical deformation, and hydration, information on the relationship between thermal properties and the microstructure and dynamics of ionic multiplets was obtained. The result indicates that the low-temperature DSC peak is not directly related to changes of ionic multiplets but related to crystallites in proximity of the multiplets.

## Experimental Section

**Materials.** Surlyn 8920 (E-0.054MAA-0.6Na), which contains 5.4 mol % MAA and is 60% neutralized by sodium, was used in this investigation. Samples were first heated in quartz tubes under dynamic vacuum at 423 K for 1.5 h. After that, samples were cooled under vacuum by ice water. The quenched samples were divided into four groups. The first group of samples, referred to here as quenched samples, was sealed in quartz tubes under vacuum followed by (typical delay of 1 h) DSC and NMR measurements. The second group, referred to here as relaxed samples, was sealed in quartz tubes under vacuum and was kept at room temperature for 1 month before DSC and NMR measurements. The third group, referred to here as relaxed-compressed samples, was prepared by compressing the relaxed samples with a pressure of 275 MPa for 1 min. During the compression treatment, these samples were exposed to air for about 1 h followed immediately by DSC or NMR measurements. The effect of moisture here should be negligible since we did not observe any noticeable changes by DSC and NMR in quenched-relaxed samples upon 1 h exposure to air. The fourth group, referred to here as hydrated samples, was relaxed samples placed in a desiccator under saturated water vapor at room temperature for 4 days. Water uptake in these samples was determined by weight increase as a function of time. The water uptake in the hydrated samples after 4 days of hydration is 2.6 wt %, corresponding to 1.4  $\text{H}_2\text{O}$  molecules per  $\text{Na}^+$  ion. The saturated level of water uptake is 7.9 wt %, which corresponds to 4.2  $\text{H}_2\text{O}$  molecules per  $\text{Na}^+$  ion.

**Measurements.** DSC measurements were carried out using Perkin-Elmer Pyris 1 with a scanning rate of 10 K/min. Indium and tin were used as calibration standards. NMR measurements were carried out using pulsed spectrometers. Unless

\* Corresponding author. E-mail: yuewu@physics.unc.edu.

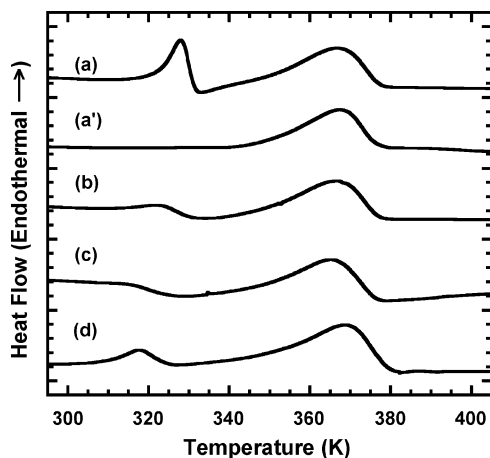


**Figure 1.** DSC results for various samples: (a) relaxed sample; (a') second heating of relaxed sample; (b) quenched sample; (c) relaxed-compressed sample; (d) hydrated sample.

explicitly mentioned, results were obtained at a magnetic field of 9.4 T. For studying field dependence some spectra were recorded at a magnetic field of 4.7 T. Dilute aqueous NaCl solution was used as  $^{23}\text{Na}$  chemical shift reference. The typical nonselective  $90^\circ$  pulse is  $4.3 \mu\text{s}$  as determined in aqueous NaCl. With selective excitation,  $^{23}\text{Na}$  spectra were recorded using either one pulse or Hahn echo sequence ( $90^\circ-t-180^\circ-t$ -detection). An Oxford continuous flow cryostat was used for NMR measurements at and below room temperature, and a homemade high-temperature probe was used for measurements at and above room temperature.

## Results and Discussion

**DSC.** Figure 1 shows the DSC curves of the various samples examined in this study. The first heating curve of the relaxed sample shows the two characteristic endothermic peaks, one at 329 K and the other at 364 K. The second heating curve, followed immediately after the first, only shows the peak at 364 K. As is well-known, the peak at 329 K reappears after a certain time of structural relaxation at room temperature. As expected, the quenched sample shows only a very weak endothermic peak at 323 K along with the higher temperature endothermic peak. Since a delay of 1 h occurred after quenching before the DSC measurement was carried out for the quenched sample, partial recovery of the low-temperature endothermic peak took place. This peak grows in intensity and moves to higher temperature as a function of relaxation time. As reported earlier, no further change occurs after 30 days of relaxation. Figure 1 shows that hydration has a significant effect on the low-temperature endothermic peak as reported earlier.<sup>14</sup> The peak intensity decreases and the peak position moves to lower temperature at 317 K upon hydration. Similarly, compression also has a dramatic effect on this low-temperature peak which nearly disappeared after compression, as shown in Figure 1.

**NMR.** Figure 2 shows the  $^{23}\text{Na}$  NMR spectra at 190 K. The spectra of quenched, relaxed, and relaxed-compressed samples are all identical within errors with line width at half-height (LWHH) of  $9.5 \pm 0.3$  kHz. The hydrated sample is narrower with LWHH of  $8.4 \pm 0.3$  kHz. Figure 3 shows the temperature dependence of the line width of the nonhydrated samples up to 580 K along with the hydrated sample data. For the hydrated sample the line width decreases rapidly above 210 K and

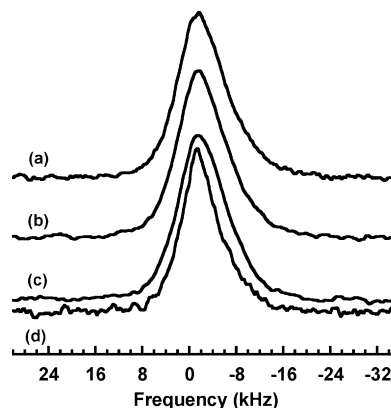


**Figure 2.**  $^{23}\text{Na}$  NMR spectra for various samples at 9.4 T and 190 K: (a) relaxed sample; (b) quenched sample; (c) relaxed-compressed sample; (d) hydrated sample.

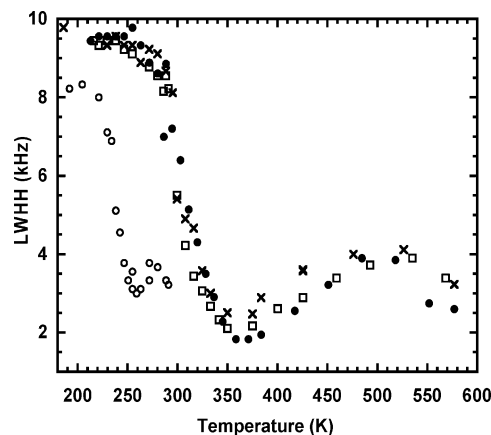


**Figure 3.**  $^{23}\text{Na}$  LWHH (line width at half-height) for various samples vs temperature: (●) relaxed sample; (×) quenched sample; (□) relaxed-compressed; (○) hydrated sample.

reaches a minimum value of  $3.0 \pm 0.3$  kHz at 255 K. Upon further increase of temperature, the motional narrowing is followed by a slight increase of the line width to  $3.7 \pm 0.3$  kHz at 275 K (possibly due to motions with rate becoming comparable to  $^{23}\text{Na}$  Larmor frequency<sup>17</sup> of 105.76 MHz) and then drops again to  $3.2 \pm 0.3$  kHz upon further heating. For the three nonhydrated samples the line width decreases dramatically above 300 K instead of 210 K in the hydrated sample. It drops to a minimum of 2.5 kHz at 375 K, followed by an increase to 4.0 kHz at 500 K, where the rate of motion reaches the  $^{23}\text{Na}$  Larmor frequency,<sup>17</sup> and then drops again. Figure 3 shows clearly that the line width at 190 K is determined exclusively by the structural environment around Na atoms.

The line width at 190 K and below is determined by spin interactions including chemical shift, dipolar interactions, and quadrupolar interactions. Figure 2 shows that there are no noticeable differences in structure that are detectable by static  $^{23}\text{Na}$  spectra in the three nonhydrated samples, in contrast to the significant change in the low-temperature DSC peak upon relaxation and compression. Figure 3 shows that the three nonhydrated samples exhibit very similar line narrowing behavior in the temperature range of 320–330 K where the low-temperature DSC peak appears. This indicates that molecular motions of ionic multiplets are not affected significantly by relaxation or compression. Moreover, the  $^{23}\text{Na}$  line width of nonhydrated samples is reversible vs measurement temperature

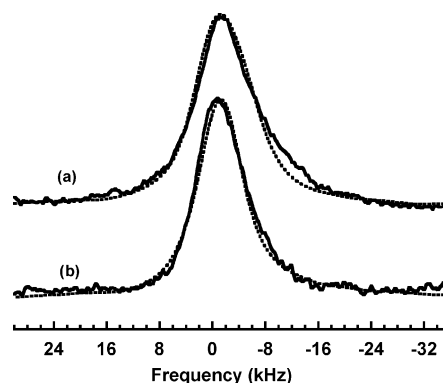


**Figure 4.**  $^{23}\text{Na}$  NMR spectra for hydrated sample at 190 K in field of 9.4 and 4.7 T and simulation curves (dotted lines): (a) 4.7 T, LWHH = 10.7 kHz; (b) 9.4 T, LWHH = 8.4 kHz.

whereas the low-temperature DSC peak has a very long relaxation time and recovers fully only after a few weeks of relaxation at room temperature. Thus, the change of the low-temperature DSC peak is not directly related to either structural changes, such as order–disorder transition, or changes of dynamical properties of ionic multiplets. On the other hand, when ionic multiplets are affected by hydration as evidenced by  $^{23}\text{Na}$  NMR, the low-temperature DSC peak also shows significant change. This is consistent with the picture that the low-temperature DSC peak is related to structure in proximity to ionic multiplets. Similar conclusion was drawn on the basis of other experiments.<sup>13</sup>

One of the connections between  $^{23}\text{Na}$  NMR spectra and structure is through quadrupole interactions. Figure 4 shows the  $^{23}\text{Na}$  NMR spectra of the hydrated sample at 190 K obtained at magnetic fields of 4.7 and 9.4 T. The line width at 4.7 T is 10.7 kHz, which is broader than that at 9.4 T, a clear indication that the second-order quadrupole broadening contributes significantly to the line width. The observed NMR signal is the  $1/2 \leftrightarrow -1/2$  central transition of  $^{23}\text{Na}$  spin  $I = 3/2$  nuclei. The contribution of the quadrupole interaction to the resonance frequency in hertz is given by<sup>18</sup>

$$\Delta\nu\left(\frac{1}{2} \leftrightarrow -\frac{1}{2}\right) \propto -\frac{3\chi^2}{2[2I(2I-1)]^2\nu_L}$$

Here,  $\nu_L = \gamma_I B/2\pi$  is the Larmor frequency determined by the external magnetic field  $B$  and the gyromagnetic ratio  $\gamma_I$ .  $\chi = e^2qQ/h$  is the nuclear quadrupolar coupling constant determined by the nuclear quadrupole moment  $Q$  and the magnitude of the electric field gradient  $eq$ . Another parameter determining the line shape is the asymmetry parameter  $\eta$ , which describes the deviation of the electric field gradient (EFG) tensor from axial symmetry. The observed  $^{23}\text{Na}$  spectra observed at 4.7 and 9.4 T can be fit (line shape simulations by SIMPSON<sup>19</sup> of both spectra shown in Figure 4) with  $\chi = 1.71$  MHz and  $\eta = 0.5$ , as shown in Figure 4. The narrower line width of the hydrated sample at 190 K compared to that of nonhydrated samples indicates that hydration causes reduction of the EFG at Na sites.

As mentioned earlier, hydration has a significant effect on motional narrowing of  $^{23}\text{Na}$  line width above 210 K. To investigate the mechanism of such effect, the transverse magnetic relaxation was measured by Hahn-

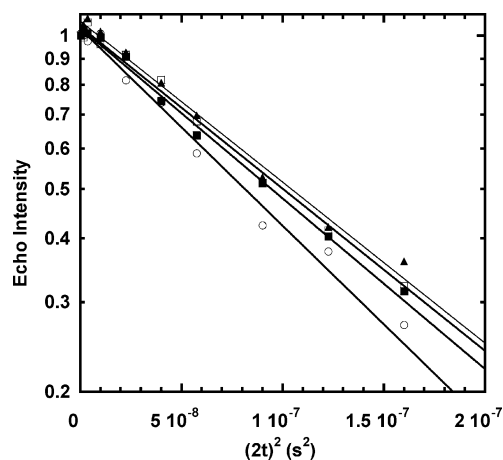


**Figure 5.** Time dependence of the Hahn-echo intensities of various samples at 260 K: (▲) relaxed sample,  $M_{2E} = 1.45 \times 10^7 \text{ s}^{-2}$ ; (■) quenched sample,  $M_{2E} = 1.54 \times 10^7 \text{ s}^{-2}$ ; (□) relaxed-compressed sample,  $M_{2E} = 1.46 \times 10^7 \text{ s}^{-2}$ ; (○) hydrated sample,  $M_{2E} = 1.78 \times 10^7 \text{ s}^{-2}$ .

echo decay. The Hahn-echo intensity  $S$  vs  $t$  is described by<sup>18</sup>

$$S(2t) \propto \exp[-M_{2E}(2t)^2/2]$$

If the effect of motion is negligible,  $M_{2E}$  is determined solely by dipole–dipole interactions. For “semi-like spins” (which are subject to different quadrupole couplings but the same central transition frequency) and selective excitation of the central transition,  $M_{2E}$  is given by<sup>18</sup>  $M_{2E} = 0.5M_2$ .  $M_2$  is the second moment determined by dipole–dipole interactions given by<sup>20</sup>

$$M_2 = \frac{9}{5} \left( \frac{\mu_0}{4\pi} \gamma_I^2 \hbar \right)^2 \frac{1}{N} F_{\text{SL}}(I) \sum_{i,k} \frac{1}{r_{ik}^6}$$

Here,  $F_{\text{SL}}(I) = 1$  for  $I = 3/2$ ,  $N$  is the number of interacting  $^{23}\text{Na}$  nuclear spins, and the summation is over all pairs of  $^{23}\text{Na}$  nuclei  $i$  and  $k$  with distance  $r_{ik}$ . The intensities  $S(2t)$  are plotted on a log scale as a function of  $(2t)^2$  ( $\text{s}^2$ ) and will yield straight lines at short  $t$  if dipolar interactions dominate the decay.

Figure 5 shows the Hahn-echo decay curves of quenched, relaxed, relaxed-compressed, and hydrated samples at 260 K. Within errors, all the nonhydrated samples have the same value of  $M_{2E}$ , and the hydrated sample has a slightly larger  $M_{2E}$ . A possible reason for the slightly larger  $M_{2E}$  for the hydrated sample is that the excitation might be slightly nonselective due to the smaller quadrupolar interaction. Using the measured second moment and assuming a multiplet consisting of 13 Na and 13 O atoms with a NaCl-type structure, the nearest-neighbor Na–Na distance  $d_{\text{Na–Na}}$  can be estimated. Such estimated Na–Na distance, the corresponding Na–O distance  $d_{\text{Na–O}}$ , and the measured  $M_{2E}$  value are listed in Table 1 for the four samples. For nonhydrated samples, based on NaCl-type structure,  $d_{\text{Na–Na}}$  of 3.17 Å is derived yielding a distance  $d_{\text{Na–O}}$  between Na and O of  $3.17/\sqrt{2} = 2.24$  Å. The identical  $M_{2E}$  values of the nonhydrated samples indicate that ionic multiplets remain unchanged after long time relaxation or compression. The calculated Na–O distance increases slightly if larger multiplet is considered. In the limit of an infinite NaCl-type lattice (this is of course not a real multiplet), the calculated  $d_{\text{Na–Na}}$  and

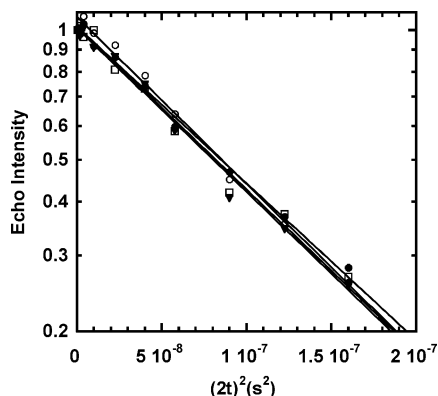


**Figure 6.** Hahn-echo decay curves of hydrated sample at 198, 220, 240, and 260 K: (○) 198 K,  $M_{2E} = 1.78 \times 10^7 \text{ s}^{-2}$ ; (▼) 220 K,  $M_{2E} = 1.75 \times 10^7 \text{ s}^{-2}$ ; (●) 240 K,  $M_{2E} = 1.72 \times 10^7 \text{ s}^{-2}$ ; (□) 260 K,  $M_{2E} = 1.78 \times 10^7 \text{ s}^{-2}$ .

**Table 1.**  $M_{2E}$  Values, the Calculated Na–Na Distances  $d_{\text{Na–Na}}$ , and the Corresponding Na–O Distances  $d_{\text{Na–O}}$

sample	temp (K)	$M_{2E} (\times 10^7 \text{ s}^{-2})$	$d_{\text{Na–Na}} (\text{Å})$	$d_{\text{Na–O}} (\text{Å})$
quenched	260	$1.54 \pm 0.06$	$3.14 \pm 0.04$	$2.22 \pm 0.03$
	303	$2.3 \pm 0.3$	N/A	N/A
	316	$4.0 \pm 0.7$	N/A	N/A
relaxed	260	$1.45 \pm 0.08$	$3.17 \pm 0.05$	$2.24 \pm 0.04$
relaxed-compressed	260	$1.46 \pm 0.08$	$3.17 \pm 0.05$	$2.24 \pm 0.04$
hydrated	198	$1.78 \pm 0.09$	$3.07 \pm 0.05$	$2.17 \pm 0.03$
	220	$1.75 \pm 0.09$	$3.08 \pm 0.05$	$2.18 \pm 0.03$
	240	$1.72 \pm 0.08$	$3.08 \pm 0.05$	$2.18 \pm 0.03$
	260	$1.78 \pm 0.09$	$3.07 \pm 0.05$	$2.17 \pm 0.03$

$d_{\text{Na–O}}$  are 3.57 and 2.52 Å, respectively. Compared to the well-known ionic radius of Na and O, 1.02 and 1.4 Å, respectively, the measured Na–Na distance  $d_{\text{Na–Na}}$  agrees very well with multiplet structures with close-packed  $\text{Na}^+ - \text{O}^-$  ionic pairs.

For the hydrated sample,  $M_{2E}$  values were also measured at temperatures where the dramatic line narrowing occurs. Figure 6 shows the Hahn-echo decay curves of hydrated sample at 198, 220, 240, and 260 K, where the dramatic line narrowing occurs. Surprisingly, the slope of the echo decay remains unchanged over this temperature range despite the significant line narrowing. This shows clearly that the atomic motion which leads to the initial reduction of the line width is of much higher frequency compared to the time scale of the transverse relaxation. For instance, vibrations of water molecules around Na atoms could cause such changes. Another evidence of such fast motions is given by the spin–lattice relaxation time. At 170 K,  $T_1$  is 39.5 ms, which decreases quickly to 7.7 ms at 220 K. Since motion-induced spin–lattice relaxation is most effective for motions with frequency approaching the Larmor frequency, it is too fast to be detected by the transverse relaxation which has the time scale of a few hundred microseconds. The onset of this NMR-detected fast motion of water molecules could eventually lead to other mode of motions of water molecules, such as those detected by dielectric loss measurement,<sup>21</sup> which contributes further to motional narrowing.

Figure 7 shows the Hahn-echo decay curves of the quenched sample at 260, 303, and 316 K, which are the characteristic temperatures over the range of the dramatic line narrowing. The decay rate of the Hahn echo starts to increase gradually above 260 K. Here, the motion contributing to motional narrowing also contrib-

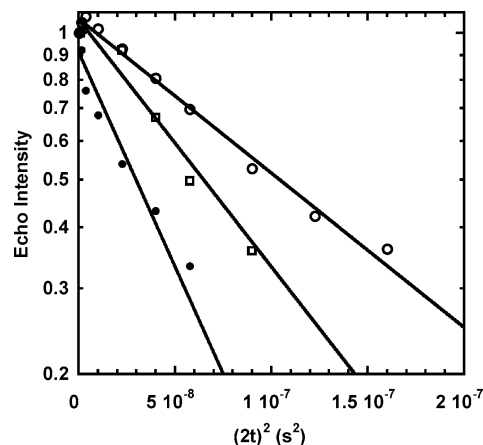


**Figure 7.** Hahn-echo decay curves of the quenched sample at 260, 303, and 316 K: (○) 260 K,  $M_{2E} = 1.54 \times 10^7 \text{ s}^{-2}$ ; (□) 303 K,  $M_{2E} = 2.3 \times 10^7 \text{ s}^{-2}$ ; (●) 316 K,  $M_{2E} = 4.0 \times 10^7 \text{ s}^{-2}$ .

utes to the decay rate of the Hahn echo, unlike in the hydrated sample below 260 K. Therefore, this is attributed to the typical onset of slow motion with increasing rate as temperature increases. The time scale of such slow motion, which causes changes of Na local environment (thus the resonance frequency of  $^{23}\text{Na}$ ), becomes comparable to the transverse relaxation time scale of a few hundred microseconds associated with dipolar interactions and causes additional decay of the Hahn echo. Therefore, the decay rate of the Hahn echo reflects not only dipole–dipole interactions but also slow motion. This shows clearly that the line narrowing of the quenched sample above 300 K is due to slow motions of  $\text{Na}^+$  ions, such as hopping and possibly motions of the polymer backbone. The time scale of such motions is a few hundred microseconds around 300 K.

## Conclusions

The structure and dynamics of ionic multiplets were investigated by  $^{23}\text{Na}$  NMR and DSC. The low-temperature DSC peak is related to structure in proximity to ionic multiplets, instead of multiplets themselves. Under relaxation and compression, no detectable changes of structure and dynamics of ionic multiplets were observed by  $^{23}\text{Na}$  NMR, but hydration did change the local environment and dynamics of ionic multiplets. The nearest-neighbor distance between  $\text{Na}^+$  ions was determined to be 3.17–3.57 Å by NMR, which gives an estimated  $\text{Na}^+ - \text{O}^-$  distance of 2.24–2.52 Å. This agrees very well with ionic multiplet structure consisting of close-packed  $\text{Na}^+ - \text{O}^-$  ionic pairs. The time scale of Na motion, possibly hopping, was determined to be on the order of a few hundred microseconds near 300 K.

**Acknowledgment.** This work is supported by the NASA University Research, Engineering and Technology Institute on Bio Inspired Materials (BIMat) under Award No. NCC-1-02037.

## References and Notes

- (1) Yoshimizu, H.; Tsujita, Y. *Annu. Rep. NMR Spectrosc.* **2001**, *44*, 1–22.
- (2) Hirasawa, E.; Yamamoto, Y.; Tadano, K.; Yano, S. *Macromolecules* **1989**, *22*, 2776–2780.
- (3) Hirasawa, E.; Yamamoto, Y.; Tadano, K.; Yano, S. *J. Appl. Polym. Sci.* **1991**, *42*, 351–362.
- (4) Fall, R. Virginia Polytechnic Institute and State University in partial fulfillment of the requirements for the degree of Masters of Science in Chemistry, 2001.

- (5) Kalista, S. J., Jr.; Ward, T. C.; Oyetunji, Z. *Proc. Annu. Meet. Adhes. Soc.* **2003**, *26*, 176–178.
- (6) Farrell, K. V.; Grady, B. P. *Macromolecules* **2000**, *33*, 7122–7126.
- (7) Grady, B. P.; Floyd, J. A.; Genetti, W. B.; Vanhoorne, P.; Register, R. A. *Polymer* **1999**, *40*, 283–288.
- (8) Kuwabara, K.; Horii, F. *J. Polym. Sci., Part B: Polym. Phys.* **2002**, *40*, 1142–1153.
- (9) Grady, B. P. *Macromolecules* **1999**, *32*, 2983–2988.
- (10) Yarusso, D. J.; Cooper, S. L. *Polymer* **1985**, *26*, 371–378.
- (11) Kutsumizu, S.; Goto, M.; Yano, S.; Schlick, S. *Macromolecules* **2002**, *35*, 6298–6305.
- (12) Kutsumizu, S.; Tadano, K.; Matsuda, Y.; Goto, M.; Tachino, H.; Hara, H.; Hirasawa, E.; Tagawa, H.; Muroga, Y.; Yano, S. *Macromolecules* **2000**, *33*, 9044–9053.
- (13) Akimoto, H.; Kanazawa, T.; Yamada, M.; Matsuda, S.; Shonaike, G. O.; Murakami, A. *J. Appl. Polym. Sci.* **2001**, *81*, 1712–1720.
- (14) Kutsumizu, S.; Nagao, N.; Tadano, K.; Tachino, H.; Hirasawa, E.; Yano, S. *Macromolecules* **1992**, *25*, 6829–6835.
- (15) Eisenberg, A.; Hird, B.; Moore, R. B. *Macromolecules* **1990**, *23*, 4098–4107.
- (16) Tadano, K.; Hirasawa, E.; Yamamoto, H.; Yano, S. *Macromolecules* **1989**, *22*, 226–233.
- (17) Vega, A. J. In *Encyclopedia of Nuclear Magnetic Resonance*; p 3874.
- (18) Freude, D.; Haase, J. In *NMR Basic Principles and Progress*; Vol. 29, pp 27–31.
- (19) Bak, M.; Rasmussen, J. T.; Nielsen, N. C. *J. Magn. Reson.* **2000**, *147*, 296–330.
- (20) Abragam, A. In *Principles of Nuclear Magnetism*; 1961, pp 112–129.
- (21) Yano, S.; Tadano, K.; Nagao, N.; Kutsumizu, S.; Tachino, H.; Hirasawa, E. *Macromolecules* **1992**, *25*, 7168–7171.

MA047647E